THE DYNAMIC INDUCED VELOCITY FIELD OF A MODEL ROTOR IN HOVER CONDITIONS

T. J. Ellenrieder, P. R. Brinson

Department of Aerospace Engineering, University of Bristol

Bristol, BS8 1TR, UK

Abstract

Results obtained from measurements of the dynamic induced velocity field beneath a model rotor are presented. The collective and cyclic pitch of a four bladed rotor of 1.54m diameter were excited at frequencies up to 1.5 times shaft speed. Flow measurements were taken using hot wire anemometry probes and a Laser Doppler Anemometer. A range of radial and vertical positions near the rotor disc were investigated.

The results are viewed against the background of theoretical dynamic inflow models and show that the dynamic induced velocity field is more complex than previously thought and primarily driven by the distribution of shed vorticity in the wake.

Analysis of the dynamic induced flow response is conducted in the frequency domain and it is found that there are significant radial and azimuthal variations which depend on the frequency of excitation. It is also observed that a change in the character of the inflow response occurs near and above the shaft speed and that vertical measuring distance from the rotor significantly affects the measured responses.

Some results for the case of cyclic excitation are also presented and these show, that contrary to momentum theory predictions, the highest induced velocities do not occur over the area of the disc where the blade pitch is at its maximum.

Introduction

The effect of dynamic inflow was first observed as a transient thrust increase occurring when collective pitch was rapidly increased. During the period of time before the induced flow has reacted to the increase in pitch, the angles of attack on the blades are not decreased by the downward induced flow. This creates a thrust transient due to the momentarily increased blade angle of attack. Similar effects can be observed with the tail rotor.

In 1953 Carpenter and Fridovitch [2] provided a theoretical model by including an apparent mass term in the inflow formulation, and hence an effective lag in the inflow response. Further developments in the modelling of dynamic inflow were made by Mangler and Squire [3], Ormiston [4,5] leading in 1981 to the Pitt and Peters [6,7] dynamic inflow model. This linked a 'uniform', 'side-to-side' and 'fore-aft' variation of the dynamic wake to the aerodynamic loading of the rotor, for flight ranging from hover to full forward flight.

A thorough review of dynamic inflow modelling is given by Peters, Gaonkar, and Ellenrieder [8,9,10]. Chen and Hindson [11] examined the effect of inflow dynamic on the vertical and flapping response of the rotor, which was extended and compared with experimental data from a hover stand by Ellenrieder and Brinson [12]. Deficiencies in Inflow models were highlighted by Houston [13] during comparisons of theoretical models with flight test data in 1989. The popular Pitt and Peters dynamic inflow model was further extended by HaQuang [14] and Su [15], to allow for a more complex aerodynamic loading.

Recently, problems which have been attributed to dynamic inflow have been encountered with high gain fly-by-wire height hold systems [1]. Dynamic inflow also introduces couplings between the roll and pitch that have previously not been included in helicopter mathematical models.

Much of the work in the area of dynamic inflow has high lighted the lack of experimental data on the dynamic inflow response [8,16,17,18]. Previous work has also suggested that in order to isolate the induced flow response a rotor restrained in vertical movement and accurate rotor excitation over a large frequency range would be advantageous [11,18]. The experimental data presented in this paper has thus been derived from a rotor mounted on a hover stand with collective and cyclic inputs to the rotor up to and above rotor shaft frequency.

Apparatus

The experimental facility consists of a four-bladed rotor of 1.54m diameter that is driven by a hydraulic motor at speeds of up to 1600 rpm. A fully actuated swashplate and associated control system allow the collective and cyclic pitch of the rotor to be changed at frequencies up to 30 Hz. Strain gauges mounted on the blades are used

to measure blade deflection, shaft encoders provide rotor azimuth position and hot wires are used for flow measurements. A comprehensive description of the facility is given by Brinson [19] and Ellenrieder [9].

The blade has Göttingen 436 section with 60mm constant chord and no twist. The active length of the blade from the tip to root attachment is 0.70m, with an approximate two dimensional lift curve slope of 6 per radian. The blade is mounted in the hub without any mechanical flap or lag degree of freedom and the pitch of the blade is directly controlled by pitch links to a conventional swash plate. The weight of the blade is 0.171 Kg/m and it is balanced so that its centre of gravity coincides with the centre of lift at the quarter-chord point. The normal operating point of the rotor is 1200 rpm giving a tip speed of 97 m/s, with a nominal root pitch setting of 12 degrees. Inflow measurements are taken radially at a distance of 15 cm below the rotor plane. All of the results presented in this paper are for the nominal operating point except where otherwise stated.

The need for tight rotor speed control in examining the dynamic induced velocity field was highlighted by Houston [20,18] and for the purposes of this work an aggressive speed control loop is used [9].

It is not possible to directly measure the thrust generated from the rotor, but estimates using a rotor performance program suggest a lift of 300 N and thrust coefficient of 0.014, at the nominal operating point.

The inflow measurements were predominantly made using hot wire anemometry probes mounted on a rake beneath the rotor. Fig. 1 shows a schematic of the basic rotor geometry and gives the location of the measuring points.

Some time series inflow results were obtained using a Laser Doppler Anemometer (LDA). Operational problems with the LDA restricted its use, but the LDA did provide an independent check on the validity of the hot wire data and also served to confirm the hot wire calibration.

Fig. 2a shows a close up of the base plate and hub assembly and Fig. 2b shows the rotor mounted in the wind tunnel. Most of the measurements were taken on the aerodynamically clean starboard side.

To examine the induced velocity behaviour, the rotor was excited at a range of discrete frequencies. From the data collected, the gain and phase frequency responses of the inflow with respect to the inputs on the rotor were established. A correlation procedure was used to extract the gain and phase shapes and record lengths were chosen such as to enable good repeatability in the presence of poor signal to noise ratios.

The inputs to the rotor for both the collective and cyclic excitation consisted of root pitch changes of peak amplitude 1.43 degrees. The frequency responses are given as Bode plots, with the gain shown in Decibels.

Dynamic Inflow Field

Collective Excitation The gain and phase responses averaged over 5 runs, together with the standard deviation, are shown in Fig. 3. Of the 12 radial positions examined only three representative cases (41%, 57% and 73%) of the full data set are shown. All of the frequency responses show reasonably flat gain shapes in the region 0.5 Hz to 10 Hz followed by a drop in gain at around 10 Hz and subsequent recovery.

Figure 4 shows the gain of the dynamic inflow response plotted against radial station for a selection of 6 frequencies from the complete data set. Again, the average of 5 runs together with the standard deviation is shown. Clearly, the dynamic inflow distribution is not constant with radius and it also changes significantly with frequency. As excitation frequency is increased, the inflow response becomes more concentrated in the region around 80% R. At high frequencies the inflow near the outer section of the blade continues to respond to pitch changes on the rotor. The phase plots show an interesting sharp recovery in phase in the region of 20-24 Hz, which becomes more pronounced for radial stations of 49% R and outwards.

The variation of the induced inflow phase with radius is shown in Fig. 5. The upper graph shows the low frequency cases and the lower graph the high frequency cases. The rate at which the phase decays towards the inboard section of the blade increases with frequency. With increasing frequency the inflow phase lag at a radial station generally increases, together with a trend of increasing inflow phase lag towards the inboard station. The variation for the higher frequencies is shown on the lower graph but is much less clear.

The experiments examining the inflow response with frequency and radial station were repeated for three rotor speeds of 1000, 1200 and 1500 rpm and the are combined as carpet plots of gain against frequency and radial station and shown in Fig. 6. Salient features of the inflow response are discussed in more detail below:

Effect of Rotor Speed Variations The effect of rotor speed on the inflow response is shown in Fig. 7 and 8. The upper graphs show the gain and phase response of the 57% span station plotted against frequency for three rotor speeds. The lower two graphs show the variation of gain and phase plotted against rotor speed. In the low frequency region, the gain can be seen to increase almost linearly with rotor speed, whereas at higher frequencies this is not the case.

These results show that there are significant changes in the character of the inflow response at high frequencies and suggest that at higher rotor speeds the air responds more rapidly to loading changes. This results is in accordance with the Pitt and Peters inflow formulation in which the apparent mass term, decreases with increasing rotor speed.

Radial and Frequency Dependencies Several effects may be contributing to the observed inflow changes with respect to radius and frequency. Among these may be Reynolds number effects. The Reynolds number of the flow as referenced to the blade at a certain radial station varies along the span of the blade, increasing linearly with radius. It is known that the lift characteristics of an aerofoil section varies with Reynolds number and this may be a contributory cause for the redistribution of the induced flow with radial station. Further work using rotor blades of different chord would help isolate this effect.

It is also known that the dynamic lift characteristics of an aerofoil depend on the non-dimensional reduced frequency of its oscillation. Work by Lal [21,22] has examined the chordwise pressure distribution of an aerofoil exited in pitch at various radial stations. It was found that the reduced frequency (product of blade chord and excitation frequency non-dimensionalised on tip speed) affects the pressure distribution. Again, because of the rotating nature of the blade the reduced frequency based on frequency of oscillation and relative airspeed over the blade will vary with radial station and excitation frequency providing a further explanation for the three-dimensional inflow changes shown in the carpet plots of Fig. 6.

Work by Liou [22] which examined the induced flow response over a radial range at one excitation frequency only, observed hysteresis when the induced flow at a point is plotted against the excitation root pitch. It is also found that this hysteresis effect diminishes towards the tip and seems to be predominantly affected by the inboard shed vorticity.

An analytical approach which tracks the time-varying shed vorticity produced by the blade excitation from each blade for several revolutions should be useful in showing how the frequency of collective excitation affects the distribution of shed vorticity in the wake, and whether this reproduces the observed radial and frequency dependent variations of the inflow gain and phase.

Vertical Measuring Position As the inflow measurements could only be made a minimum of 15 cm below the plane of the rotor to avoid physical contact between the blades and hot-wires, the effect of vertical displacement on the measured inflow response was examined. The results are shown in Fig. 9 and 10. Figure 9 shows the gain and phase variation with frequency for the 57% R station. For the gain it is interesting to note that the measurements closest to the blade show the sharpest gain reduction in the area of 20 Hz. Plotting gain at a certain frequency against vertical separation showed that at the lower frequencies the variation is essentially linear but that at frequencies above shaft speed this linearity is lost.

The lower graph of Fig. 9, shows the phase inflow frequency response. Examining the alternative presentation shown in Fig. 10, it can be seen that at frequencies below shaft speed there is a linear relationship between phase and vertical station. This is shown in the top graph of Fig. 10, with least squares error fit (LSEF) lines matched to the data. For the higher frequencies the variation is no longer linear but the gradient continues to increase in steepness with frequency.

The linear relationship between the phase lag and vertical separation and the linear frequency dependence tends to be suggestive of a transmission delay. The gradients of the vertical phase lag for each frequency are also shown in Fig. 10 and are plotted on the bottom graph against frequency, showing the linear relationship between gradient and excitation frequency. A value for the transport delay of 43 deg/m/Hz based on the mean wake velocity was theoretically determined. The experimentally measured value was 63 deg/m/Hz. Hence although a pure transmission delay presents a plausible explanation for the vertical behaviour of the wake. The value determined by experiment exceeds that which can be justified using physical arguments [9].

Cyclic Excitation The response of the induced flow field to cyclic inputs ranging from 0.5 to 30 Hz is shown in Fig. 11 to 14. The cyclic input was such that the maximum blade pitch was applied at an azimuth angle of 15 degrees and the maximum blade flapping response occurred 55 degrees later at 70 degrees. This result is consistent with the semi-rigid mounting arrangement of the blades in the hub. Fig. 11 shows the inflow gain and phase at three of the twelve radial test stations. The inflow frequency responses for the case of cyclic excitation are quite different to the collective cases, where the gains remains steady for a range of frequencies between 0.5 and 10 Hz. The underlying trend of diminishing gain with frequency in the region between 1 and 5 Hz is very interesting since this band is important from the point of view of handling and control. The inflow phase response for the cyclic case is also markedly different from the collective cases.

If a conceptual wake model based on momentum theory is used, where the local induced velocities beneath the rotor are related to the local blade loading of the rotor, then the frequency responses of the collective and cyclic cases should be similar. The only difference between the

two being that in the collective case loading changes will occur over the whole disc.

The fact that the character of the frequency responses is different for the collective and cyclic cases emphasises the need for an accurate wake model where the velocity components at any point beneath the rotor are given by the combined influence of the spiralling time varying shed vortices from all of the blades. In the collective case the loading changes due to pitch changes on all blades would cause shed vorticity of varying strength to be added to the spirals already beneath the rotor. In the cyclic case the amount of shed vorticity (vorticity due to time-varying blade lift) from each blade and added to the existing spiral will be determined both by the blade azimuth position and cyclic input. From this it would be expected that the vorticity distribution in the spiralling wake would be very different from that of the collective case and this is a very likely explanation for the observed differences in the collective and cyclic inflow frequency responses.

Figure 12 shows the gain variation with radius for the cyclic cases. The increase in inflow response near the tip region as frequency increases is similar to that of the collective case. In detail however, the responses are different. The often used theoretical approximation that the cyclic dynamic inflow responses increases linearly with radius, and is constant with frequency, is only approximately correct for the mid blade region of the lowest frequency test cases. The differences between the cyclic and collective case again point to a complex wake model of spiralling vorticity. A simple wake model where the induced flow at a point beneath the rotor disc is related to the rotor loading at that point cannot be used to explain the complex structure of the dynamic induced wake observed in these results.

The inflow gain and phase response at four azimuth positions from 0 to 90 degrees is shown in Fig 13. The average of five runs is shown obtained both in hover conditions and with a very low tunnel speeds setting (advance ratio 0.025). Clearly the inflow response changes with azimuth position. The low tunnel speed cases were run initially in an attempt to reduce the circulation in the tunnel, but even the very low tunnel setting of 2.5 m/s significantly affects the recorded inflow response, reinforcing again the strong link between the observed dynamic wake and the overall wake structure. These and the earlier results were verified with the LDA.

Finally Fig. 14 shows the inflow gain and phase plotted against azimuth at a selection of frequencies. There is no clear peak in the inflow response at the azimuth position of 15 degrees which corresponds to maximum blade pitch. Working from the assumption that the magnitude of the inflow produced by a blade is proportional to the lift produced by a blade, a sinusoidal variation of the inflow could be expected with a peak at the position where the blade loading is largest. The azimuthal inflow variation is once again dependent on frequency. It seems that the wake structure is less related to disc loading than has been assumed in some theoretical models.

Conclusion

A unique experimental facility for the study of dynamic inflow has been developed. This allows examination of the dynamic induced velocity field of a model rotor under controlled excitation over a frequency range up to 1.5 times rotor shaft speed.

The dynamic response of the induced flow field is found to be highly complex, dependent on both the radial and vertical measurement position and the frequency of excitation. At lower frequencies the vertical variation in inflow phase may be approximated using a transmission delay.

The wake description of many existing dynamic inflow models do not capture important features of the real wake. It seems that the dynamic inflow response is strongly related to the structure of the wake and the distribution of time varying, shed vorticity in the wake, and not easily reconcilable with models based on momentum theory.

Acknowledgements

This work has been supported by Westland Helicopters, Yeovil, and their technical and financial support is gratefully acknowledged. The author would also like to acknowledge the contribution made by the U.K. Defence Research Agency by supporting the development of the rotor rig.

References

1 PROUTY R.W., 1992. *Even More Helicopter Aerodynamics.* Potomac: Rotor & Wing International. Phillips Publishing Inc.

2 CARPENTER P.J., FRIDOVICH B., 1953. *Effect of a Rapid Blade Pitch Increase on Thrust and Induced Velocity Response of a full-scale Helicopter Rotor.* NACA TN3044.

3 MANGLER K.W., SQUIRE H.B., 1953. *The Induced Velocity Field of a Rotor.* Aeronautical Research Council, RM No. 2642.

4 ORMISTON R.A., 1972. *An Actuator Disc Theory for Rotor Wake Induced Velocities.* France: AGARD Specialists meeting on the Aerodynamics of Rotary Wings.

5 ORMISTON R.A., 1976. *Application of Simplified Inflow Models to Rotor Craft Dynamic Analysis.* Journal of the American Helicopter Society, **(21)** 3.

6 PITT D.M., PETERS D.A., 1981. *Theoretical Prediction of Dynamic Inflow Derivatives.* Vertica, **(5)** 2.

7 PITT D.M., PETERS D.A., 1983. *Rotor Dynamic Inflow Derivatives and Time Constants from Various Inflow Models.* 9th European Rotorcraft Forum.

8 PETERS D.A., GAONKAR G.H., 1988. *Review of Dynamic Inflow Modelling for Rotorcraft Flight Dynamics.* Vertica, **(12)** 3.

9 ELLENRIEDER T.J., 1996, *Investigation of the Dynamic Wake of a Model Rotor, PhD Thesis.* Bristol: Department of Aerospace Engineering, University of Bristol.

10 GAONKAR G.H., PETERS D.A., 1984. *A Review of Dynamic inflow and its Effect on Experimental Correlation.* California: American Helicopter Society. Second Decennial Specialists Meeting on Rotorcraft Dynamics.

11 CHEN R.T., HINDSON W.S., 1987. *Influence of Dynamic Inflow on the Helicopter Vertical Response.* Vertica **(11)** 1.

12 ELLENRIEDER T.J., BRINSON P.R., 1994. *Experimental Investigation of Helicopter Coning / Inflow Dynamics in Hover.* Amsterdam: Twentieth European Rotorcraft Forum.

13 HOUSTON S.S, 1989. *Identification of Factors Influencing Rotorcraft Heave Axis Damping and Control Sensitivity in the Hover.* Royal Aircraft Establishment. AE Technical Report 88067.

14 PETERS D.A., HAQUANG N., 1988. *Dynamic Inflow for Practical Applications.* Journal of the American Helicopter Society, **(33)** 4.

15 SU A., YOO K.M., PETERS D.A., 1992. *Extension and Validation of an Unsteady Wake Model for Rotors.* Journal of Aircraft, **(29)** 3.

16 HOUSTON S.S., BLACK C.G., 1990. *On the Identifiability of Helicopter Models incorporating Higher Order Dynamics.* Royal Aircraft Establishment. Tech Memo Fm37.

17 BRADLEY R., BLACK C.G., MURRAY-SMITH D.J., 1989. *Glauert Augmentation of Rotor Inflow Dynamics.* Amsterdam: 15th European Rotorcraft Forum.

18 LEITH D.J., BRADLY R., MURRAY-SMITH D.J., 1991. *The Identification of Coupled Flapping/Inflow Models for Hovering Flight.* 17th European Rotorcraft Forum .

19 BRINSON P.R., 1991. *Experimental Investigation of Coupled Helicopter Rotor/Body Control.* Berlin: 17th European Rotorcraft Forum.

20 HOUSTON S.S., TARTELLIN P.C., 1989. *Theoretical and Experimental Correlation of Helicopter Aeromechanics in Hover.* Royal Aircraft Establishment. Tech. Memo Fm 20.

21 LAL M.K., 1994. *Measurement Around a Rotor Blade Excited in Pitch. Part 2: Unsteady Surface Pressure.* Journal of the American Helicopter Society, **(39)** 2.

22 LIOU S.G., KOMERATH M., ET AL, 1994. *Measurements Around a Rotor Blade Excited in Pitch. Part 1: Dynamic Inflow.* Journal of the American Helicopter Society, **(39)** 2.

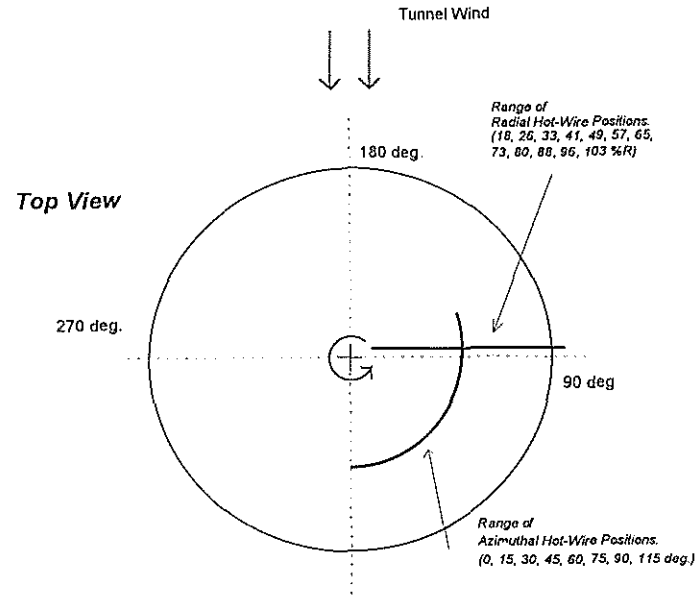

Fig. 1 Definition of basic rotor geometry and measuring positions

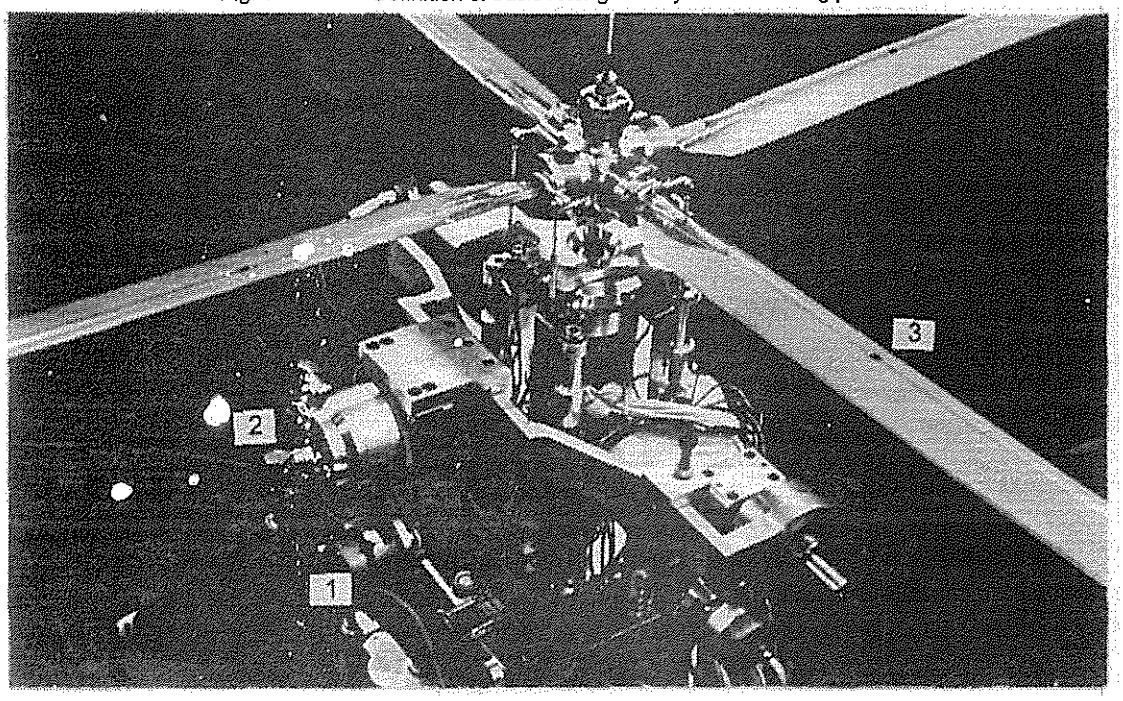

Fig. 2a Rotor and swashplate assembly

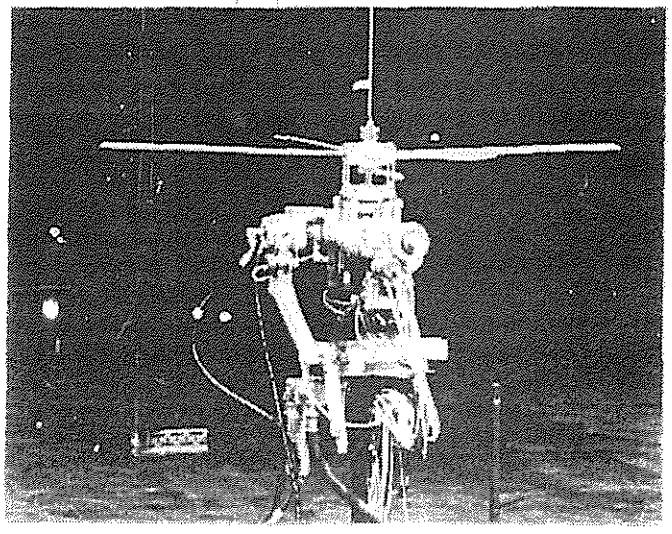

Fig. 2b Rotor mounted in the wind tunnel

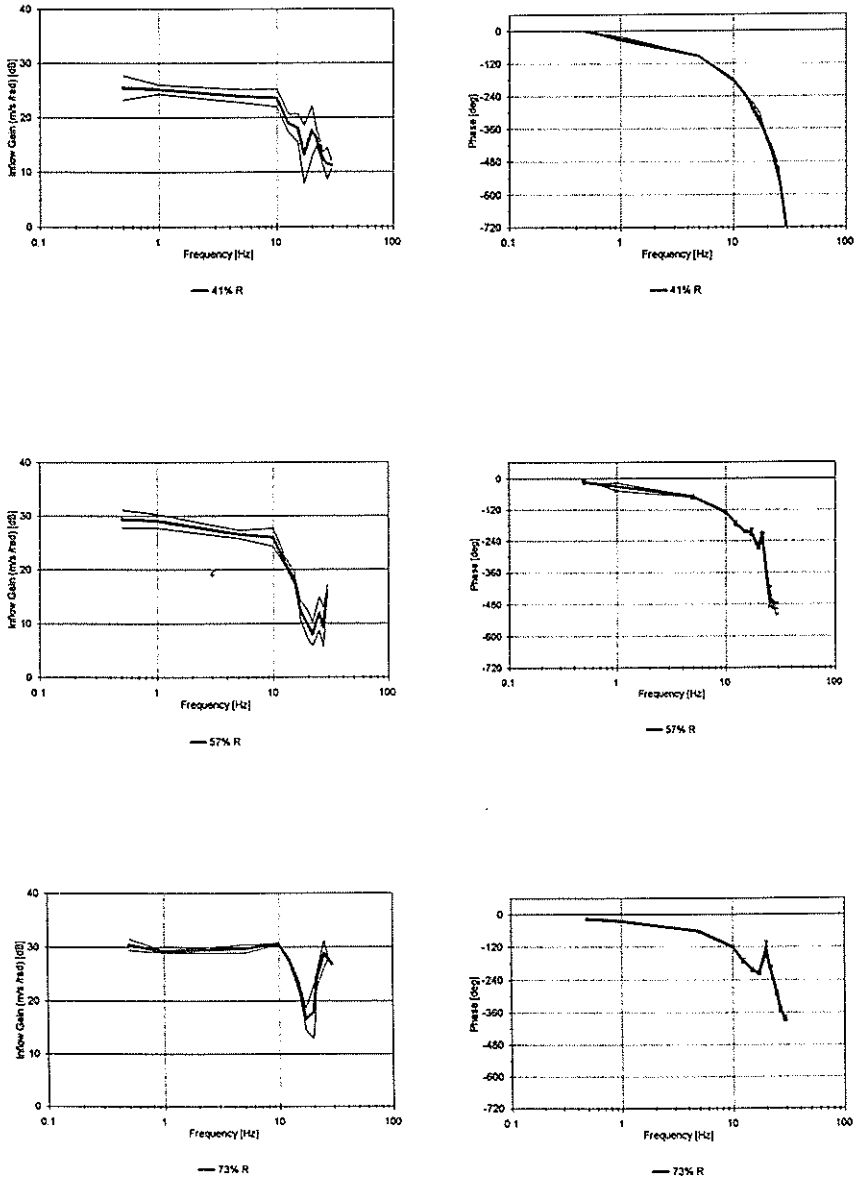

Fig. 3 Change in inflow frequency response with radial station

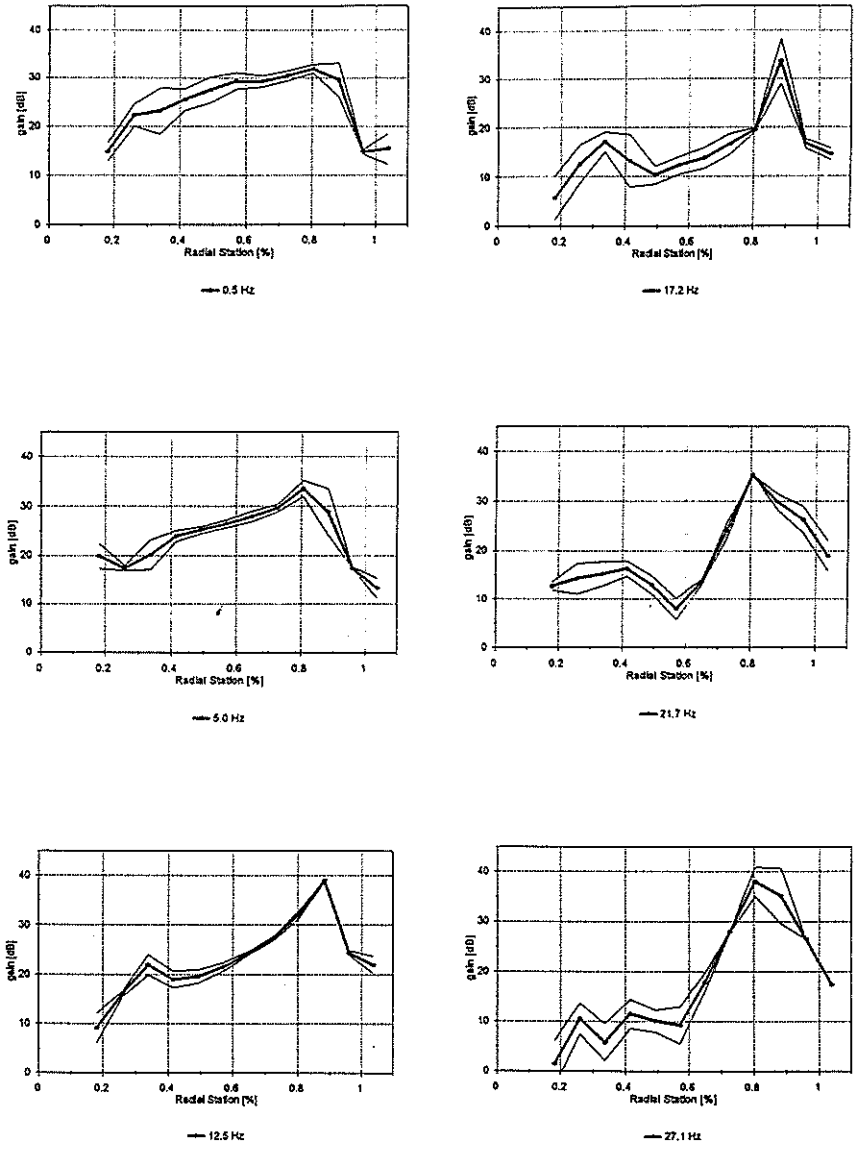

Fig. 4 Radial variation of the inflow gain at selected frequencies

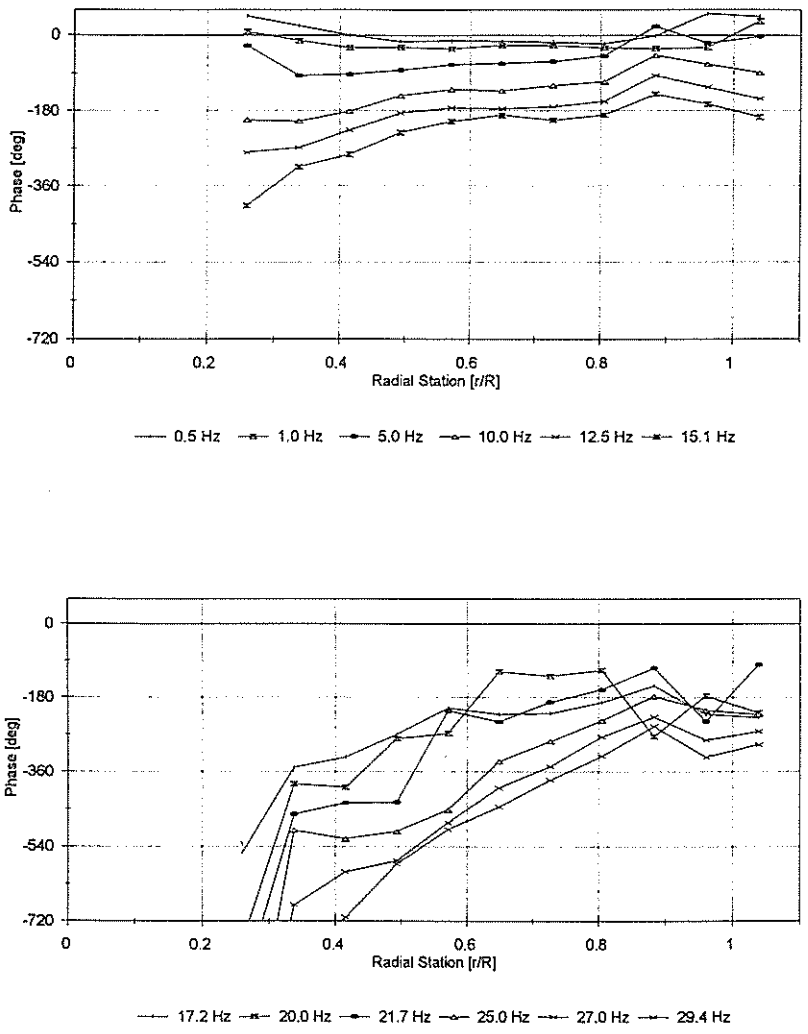

Fig. 5 Induced flow phase response with radial station

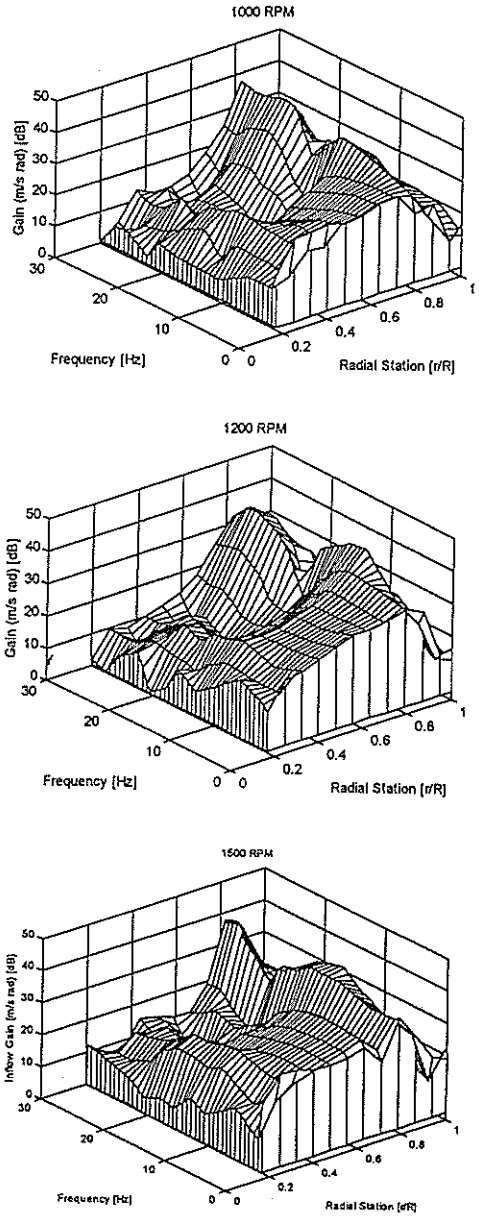

Fig. 6 Induced flow variation with frequency and radial station (1000, 1200, and 1500 rpm)

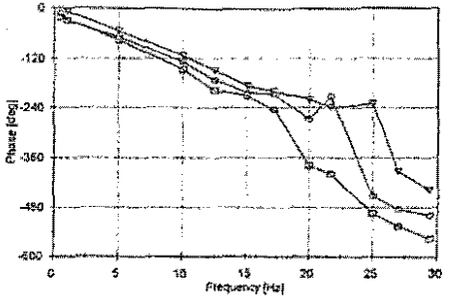

Frequency Response (1000, 1200, 1500 RPM)

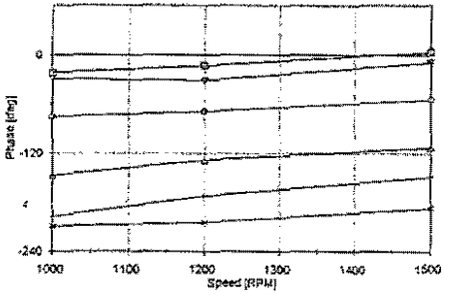

Variation with Rotor Speed (0.5-15Hz)

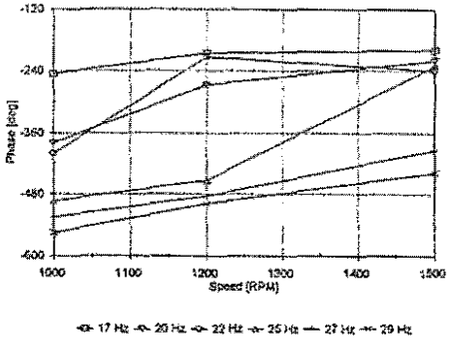

Fig. 7 Induced flow phase response variation with rotor speed at 57% R

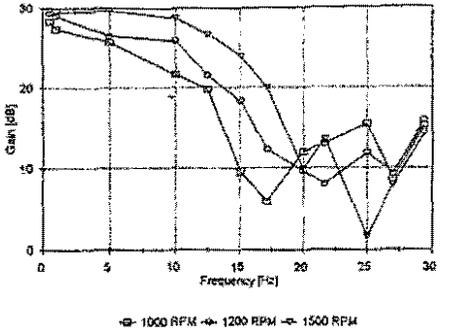

Frequency Response (1000, 1200, 1500 RPM)

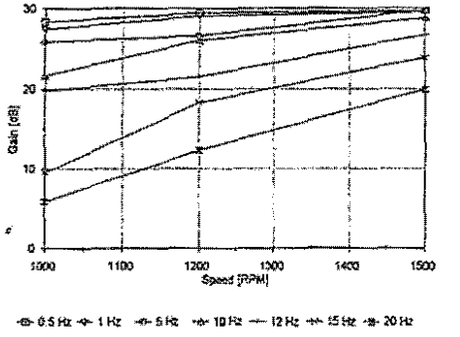

Variation with Rotor Speed (0.5-17Hz)

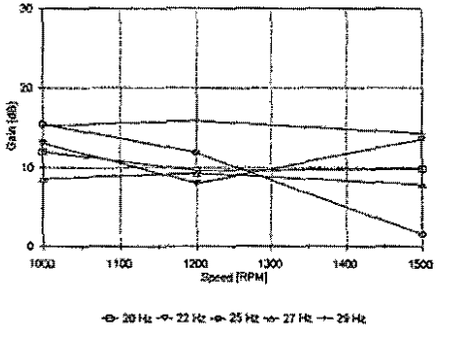

Variation with Rotor Speed (20-30Hz)

Fig. 8 Induced flow gain response variation with rotor speed at 57% R

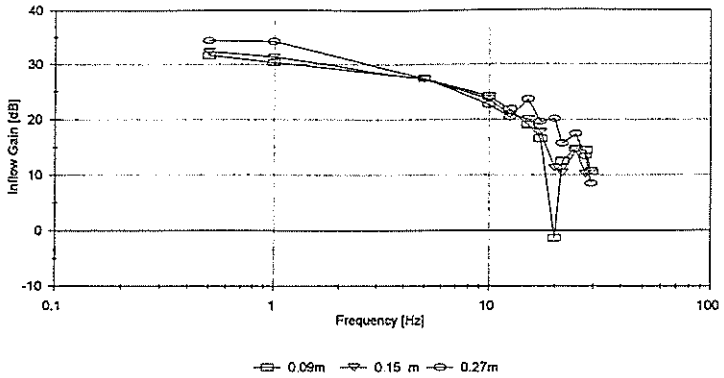

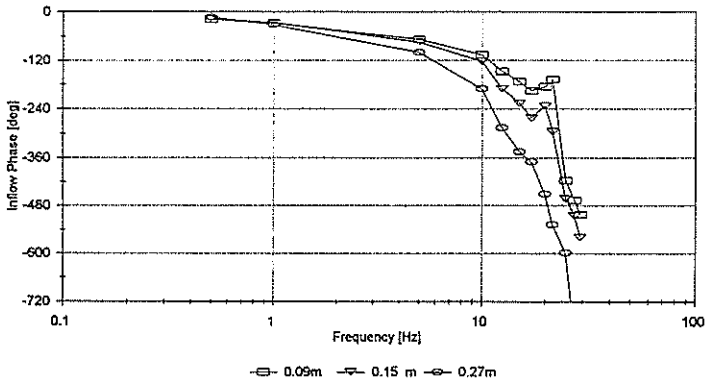

Fig. 9 Inflow gain and phase response at three vertical stations

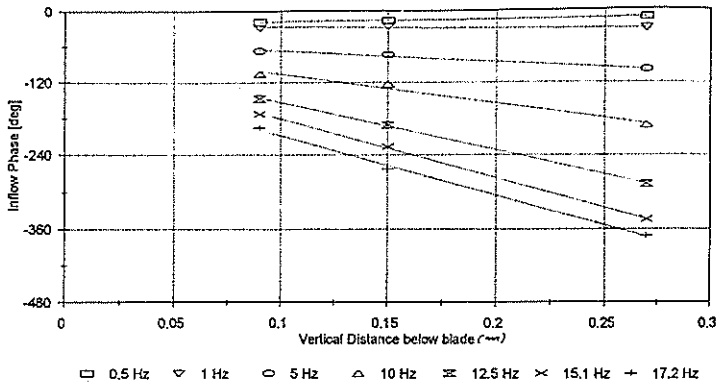

Least Squares Error Fit (LSEF) to Phase Variation

Freq. [Hz]		Gradient [deg/m	
0.5		30	
1		-25	
5		-187	
10		-483	
12.5		-779	
15.1		-959	
17.2		-966	

Table of LSEF Parameters

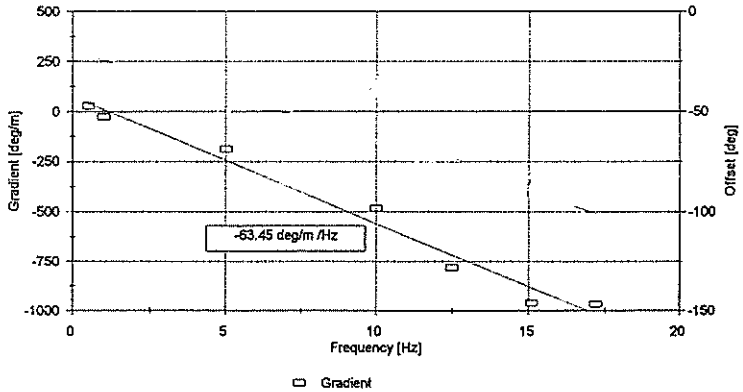

Variation of LSEF Parameters with Frequency

Fig. 10 Evidence of a transmission delay for the axial phase variation

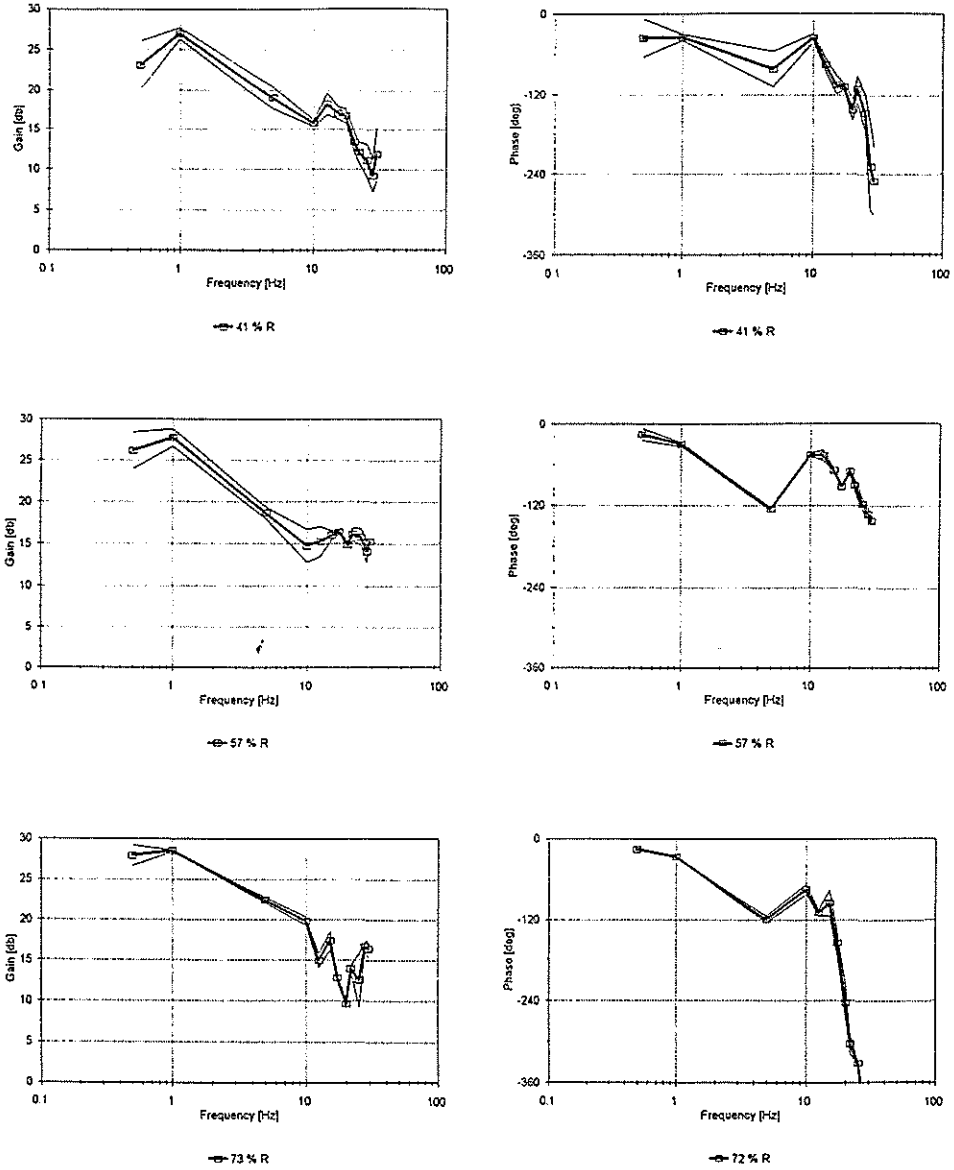

Fig. 11 Variation of the cyclic inflow response with radial station at 0° azimuth

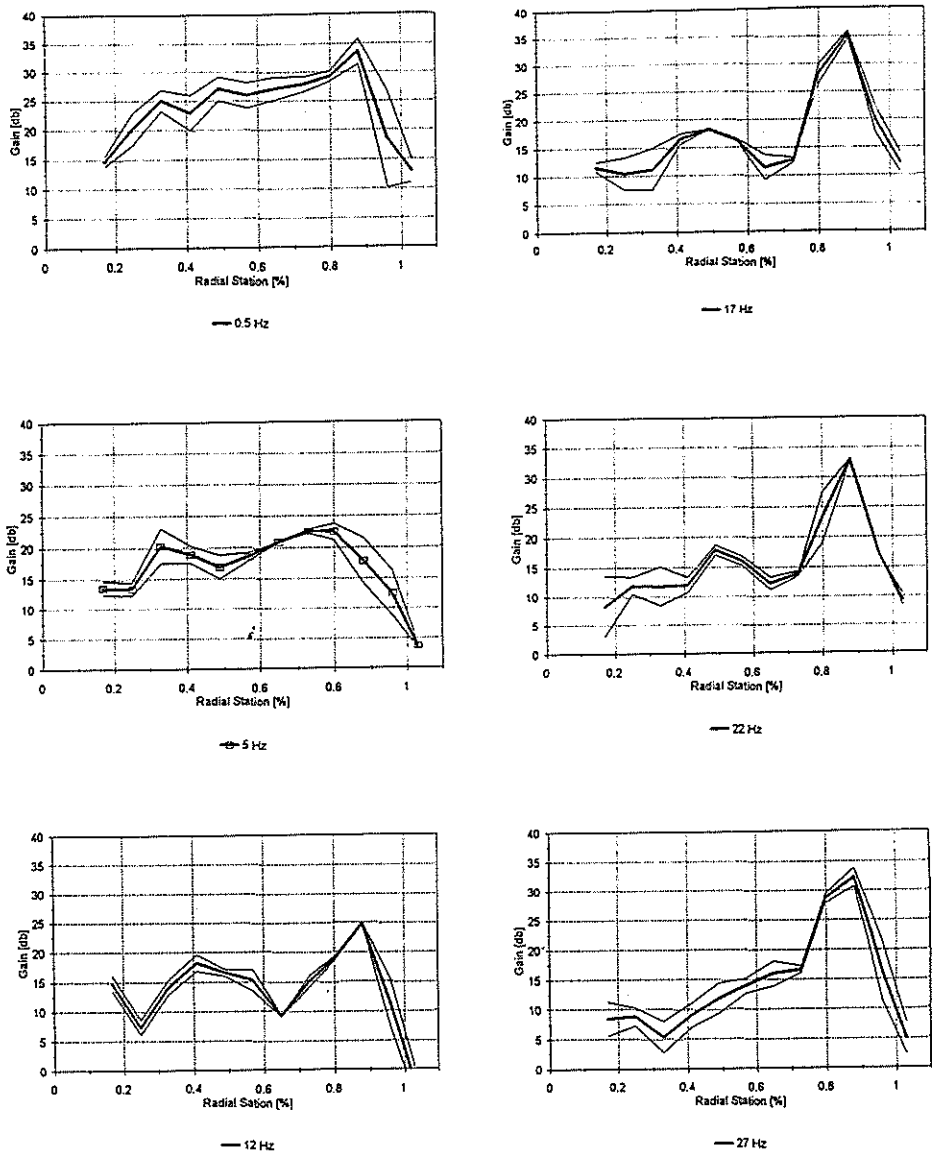

Fig. 12 Effect of frequency on the radial inflow distribution at 90° azimuth

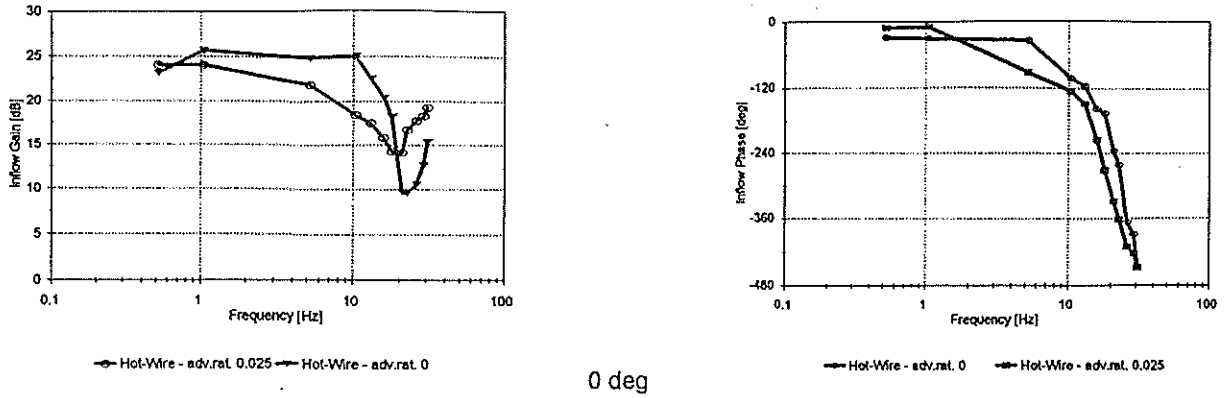

0 deg

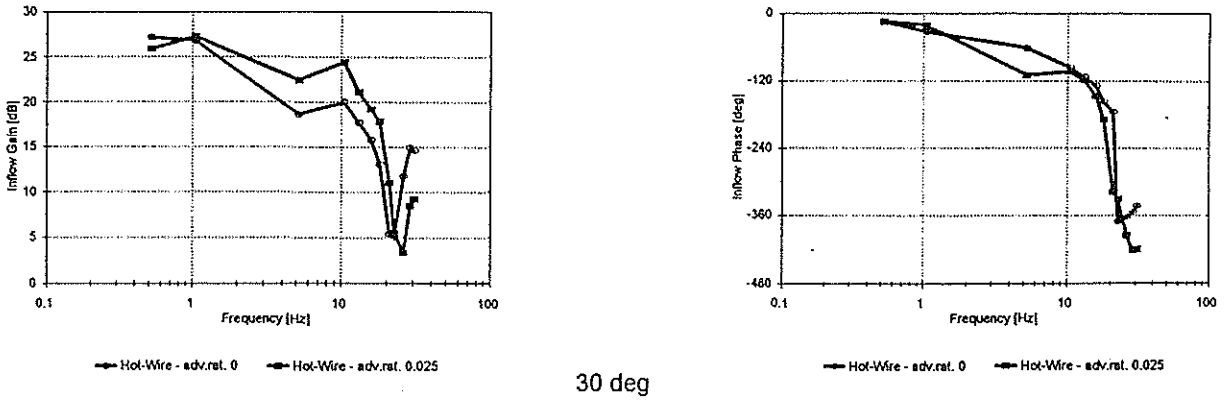

30 deg

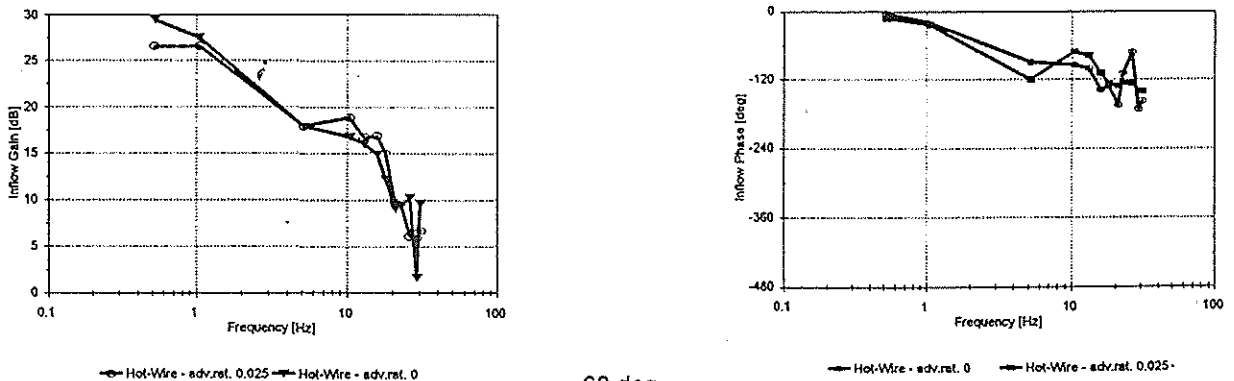

60 deg

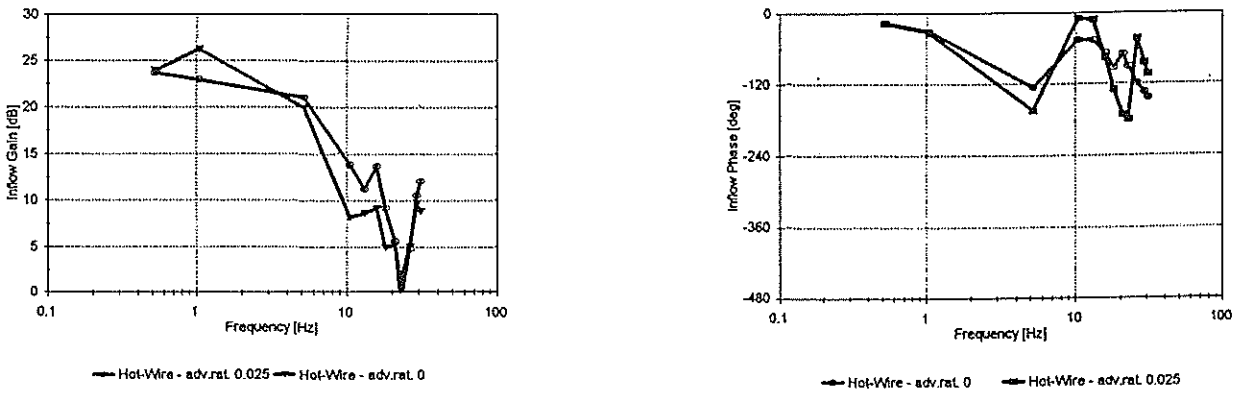

90 deg

Fig. 13 Inflow frequency response obtained at four azimuth positions

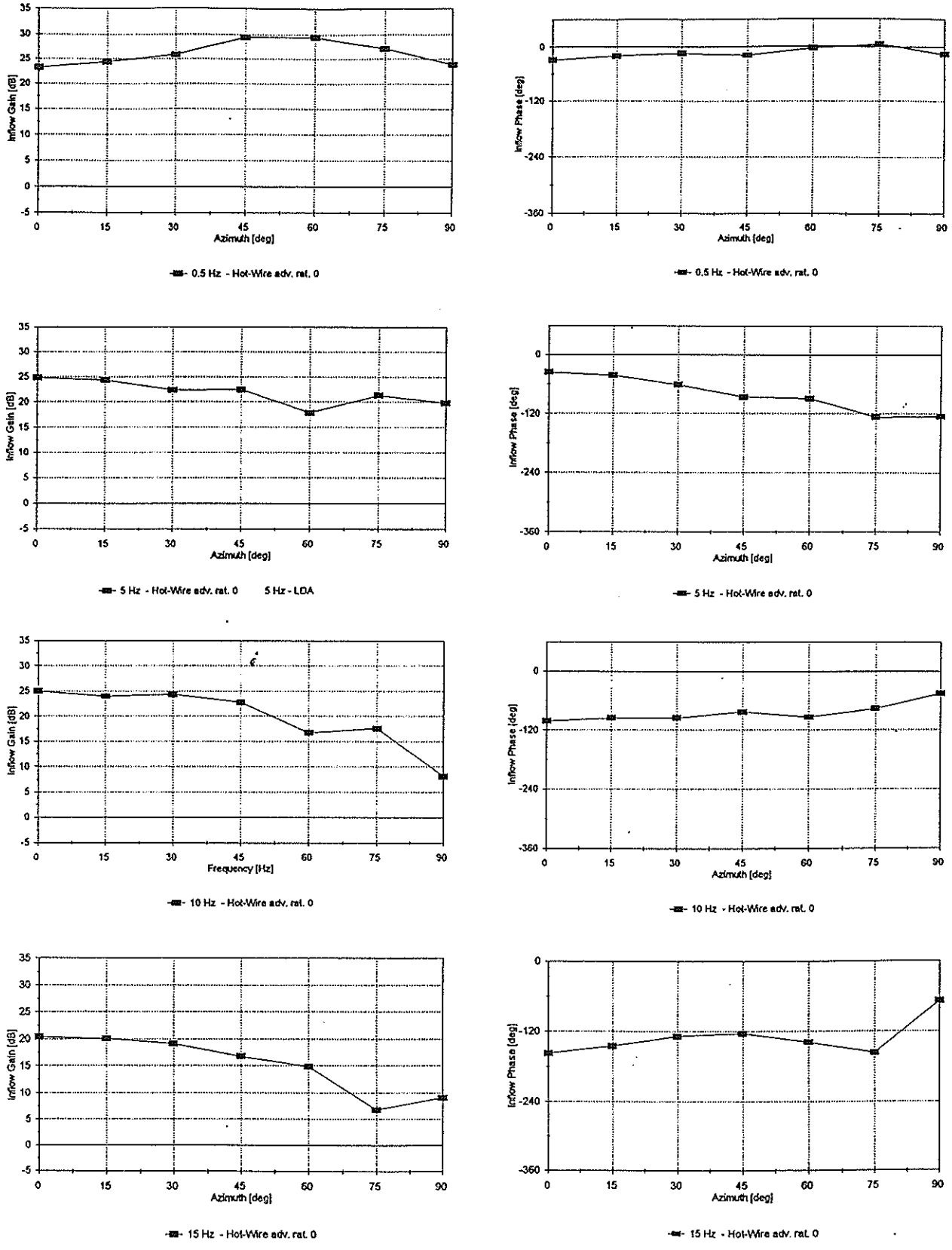

Fig. 14 Inflow response variation with azimuth at selected frequencies